



Preparation of ZnO/Cetyl Trimethyl Ammonium Salt/Hectorite as Catalyst in Alizarin Red S Photo-oxidation

IS FATIMAH

Department of Chemistry, Islamic University of Indonesia, Kampus Terpadu UII, Jl. Kaliurang Km 14, Besi, Yogyakarta, Indonesia

Corresponding author: Fax: +62 274895920; Tel: +62 896439 Ext 3002; E-mail: isfatimah@fmipa.uui.ac.id

(Received: 29 January 2011;

Accepted: 30 June 2011)

AJC-10128

Preparation of zinc oxide immobilized in cetyl trimethyl ammonium-intercalated hectorite (ZnO/CTMA/Hec) and its photocatalytic study for alizarin red S (ARS) photo-oxidation has been conducted. The synthesis of ZnO/CTMA/Hec catalyst was performed by pre-intercalation process toward synthetic hectorite followed by dispersion of ZnO *via* pillarization process. Catalyst characterization performed by XRD, surface area analyzer and energy dispersive X-ray (EDX). Activity test of material as photocatalyst in alizarin red S photo-oxidation focused on its evaluation in the alizarin red S degradation rate compared with hectorite and bulk-ZnO. The result showed that ZnO/CTMA/Hec preparation affect significantly to increase photoactivity compared to raw support; hectorite. The increase in activity was ensured from the linear correlation between catalyst dosage to the degradation rate.

Key Words: Hectorite, Pillared clays, Intercalation, Photocatalyst, Alizarin red S.

INTRODUCTION

Degradation of dyes in order to reduce the contamination to the environment is one of the efforts undertaken by some industrial users. The presence of residual dyes in industrial wastewater is one of the special attention because of the non-biodegradable nature and toxicity properties to the biota. Among several methods, photooxidation of dyes utilizing photocatalyst is one of the new technique included in the category of advanced oxidation processes (AOPs). This technique with heterogeneous photocatalyst assisted photooxidation under the the presence of active oxidants such as H_2O_2 was reported to providing a fast process and also economically benefits cause generally solid catalyst can be regenerated easily and reused¹⁻³. Semiconductor photocatalyst of TiO_2 for application of dye photooxidation was also widely reported. Its anatase phase with the high band gap energy (3.2 eV) were evaluated as the effective and non-toxic photocatalyst for water treatment purposes. Many efforts to improve TiO_2 anatase photoactivity by several method such as doping, nanosize formation and immobilization were intensively reported⁴⁻⁸. In other hand, although is also a semiconductor that can act as photocatalyst with similar band gap energy to TiO_2 , the expose of ZnO photocatalysis is less discussed. Its lower chemical stability compared to TiO_2 is probably the reason. Referred to as in TiO_2 and other photocatalyst, the use of bulk-ZnO will be ineffective compared to the inorganic matrix dispersed form. Towards environmental friendly application, ZnO immobili-

zation in a stable and porous inorganic material are hypothetically extent the feasibility of ZnO use as stable and regenerable heterogeneous photocatalyst^{9,10}. Previous research reported ZnO immobilization in some matrix such as glass plate, silica, zeolite and montmorillonite for catalyst and phtocatalyst application⁹⁻¹³. Reusable and eco-friendly properties were the noted important contribution of immobilized ZnO in solid support. Controlled particle size, specific surface area and catalyst surface morphology are also strongly affect to the molecule diffusion in the targeted reaction^{11,12}.

Smectite clay is one kind of material with properties that theoretically could be used as a support of ZnO. Smectite clay is easily sweling, modifiable and high in porosity. Previous research reported the use of montmorillonite as ZnO supporting material. Zinc oxide nanostructure in mesoporous composite materials was successfully obtained *via* the sol-gel synthesis procedure. Formation of the structure house of cards seems to be more dominant placed in it. Mesopores were formed by formation of cavity between clay sheets cause of huge ZnO particles. This structure is as reported in attaching ZnO into the montmorillonite *via in situ* immobilization and oxide formation from $ZnCl_2$ precursor¹⁴. Photoactivity test in salicylic acid photo-oxidation showed an increase in the photocatalytic activity of ZnO supported montmorillonite. As in TiO_2 pillarization, ZnO with direct pillarization into the interlayer space of smectite probably tends to damage the smectite structure as strong acid environment created within clay-precursor interaction.

In order to solve this problem, immobilization of ZnO in clay was effected by utilizing sol-gel or organometal precursor. Refer to TiO₂ immobilization within sol-gel mechanism, organic molecules-templating before ZnO impregnation or immobilization by using sol-gel ZnO precursor system is one interesting procedure to be tried. The use of alkylamine surfactant molecules including cetyl trimethyl ammonium (CTMA) salt is the most reported in templating synthesis^{15,16}.

In present research, preparation of ZnO supported smectite *via* CTMA surfactant pre-intercalation was attempted. Refer to some publications studied on the effect of CTMA intercalation to the improvement of physico-chemical character of smectite clay and the role of surfactant in creating regularity of a metal oxide formation. This new synthesis route provides some advantageous. The increasing specific surface area due to the increasing distance between the layers of clay's silicate galleries facilitates to set the distance between the incoming metal precursor neatly. Furthermore, not only as template to regulate the entry of ZnO precursors, but also to enhance the hydrophobic character of photocatalyst surface. Due to the surface properties, adsorptive capability that is theoretically close related with the increasing photocatalytic activity was proposed to be expandable through intensive interaction between the catalyst surface and target compounds in photo-oxidation reaction which is generally a non-polar organic compounds. The microwave irradiation was chosen to perform calcination step after the dispersion of zinc oxide precursor in order to maintain the CTMA molecules remain intact in clay pores while zinc precursor being oxidized¹⁷⁻²⁰.

To study the effect of preparation treatment to the physico-chemical characters and photo-activity objectively, synthetic smectite: hectorite was used. Higher crystallinity and relatively small amount of impurities within the synthetic clay sample compared to natural clays was expected to minimize the undesired interaction between precursor and clay matrix, so more accurate data will be provided to describe interactions occurred in preparation. Photo-oxidation of alizarine red S with chemical structure depicted in Fig. 1 was performed as model reaction to evaluate the activity of prepared material. In view of the role of ZnO immobilization, photo-oxidation over bulk-ZnO synthesized with analogue procedure was also carried out.

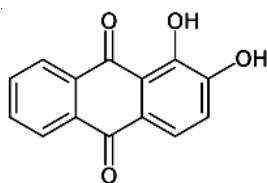


Fig. 1. Chemical structure of alizarin red S

EXPERIMENTAL

The host material *i.e.*, synthetic hectorite with the trade name of laponite was obtained from Rockwood Ltd. and used without further purification. All chemicals were in analytical grade purchased from E. Merck consist of zinc acetate dihydrate, isopropyl alcohol, cetyl trimethyl ammonium chloride and alizarine red S.

To prepare the material, CTMA pre intercalation was performed by mixing CTMA-chloride salt solution with laponite suspension in water (2 % wt.). The transparent mixture was stirred at room temperature for 24 h before was added with zinc oxide precursor made by diluting zinc acetate in isopropanol: H₂O = 50:50. The concentration of zinc loaded into hectorite was 10 % wt. Stirring to the mixture was continued for 24 h in order for interacting ZnO precursor and pre-intercalated hectorite suspension. After prolong stirring, suspension was transferred in filtration process to obtain gel. Neutralization to the gel was conducted by washing with aquadest until pH of the filtrate was equal to 7.0 before drying 75 °C in heating oven. Final step in preparation was calcination process by microwave irradiation using commercial microwave with the middle power (600 Watt) operated for 15 min. Produced material was designated as ZnO/CTMA/Hec. For characterization, instrumental analysis were conducted by using electron dispersive X-ray spectrophotometer (EDS), X-ray diffraction XRD, BET gas sorption analysis and scanning electron microscopy (SEM) observations. XRD patterns were obtained with a XRD X-6000 Shimadzu using CuK_α radiation, surface analysis for specific surface area, pore volume and pore radius were performed by using NOVA 1200e and for elemental analysis enery dispersive X-ray (EDX) JEOL JSM-7001FA.

Photocatalytic activity of the material was evaluated in photo-oxidation reaction of alizarin red-S (ARS). Photo-oxidation experiment was placed in 1 L tube reactor walled with water bath to maintain temperature of the system and the reactor was kept under UVB-lamp supplied from Philip Co. The distance between lamp and reactor system is 25 cm. Some photo-oxidation reaction series were engaged by adding photocatalyst powder to the alizarin red S solution in the reactor followed by stirring and additional H₂O₂ in small amount (5 % wt.) as oxidant. Concentration of alizarin red S in treated solution was determined by colorimetric method using UV-visible spectrophotometer HITACHI U 2080.

RESULTS AND DISCUSSION

Qualitative and comparative structure analysis was observed by XRD analysis on raw hectorite and ZnO/Hec/CTMA and from both material, similar pattern was found (Fig. 2). Diffractogram peaks at $2\theta = 5.98, 20.04$ and 35.18° are observed in hectorite which are correspond to peaks at $5.30, 20.12$ and 35.10° in Zn/CTMA/Hec, respectively.

The peaks at 5.98 and 5.30° are characteristic referring to (001) reflection and due to the shift of peak at lower angle for Zn/CTMA/Hec compared to as in hectorite, the increasing d_{001} basal spacing is concluded. As it was expected from the goal of modification, d_{001} value is 14.77 \AA for hectorite and 16.67 \AA for Zn/CTMA/Hec. Dispersion of ZnO particles in CTMA-templated clay sheets interlayer regions of clay sheets seems to be occurred in regularly basis, rather different with those reported in in previous work which describing the formation of house of cards structure¹⁴. This assumption is strengthened by the sharpness of the peak reflection (001) as measured from FWHM value (3.36°) for Zn/CTMA/Hec that is indicate the uniformly distribution of the distances between layers. The

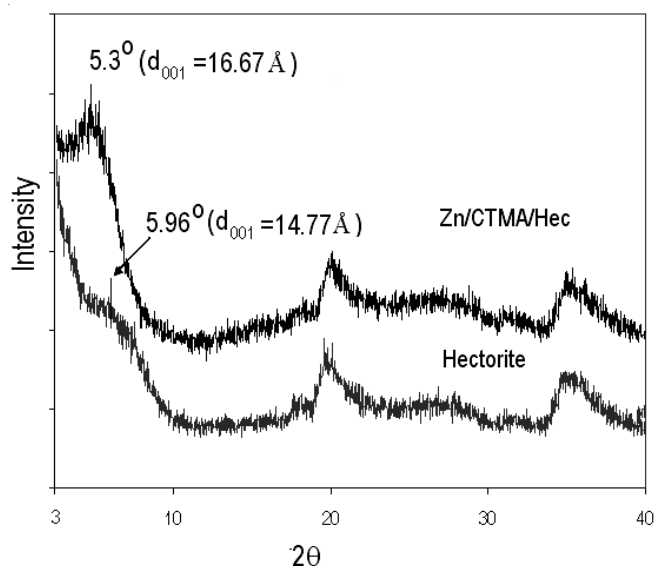


Fig. 2. XRD pattern of hectorite and ZnO/CTMA/Hec

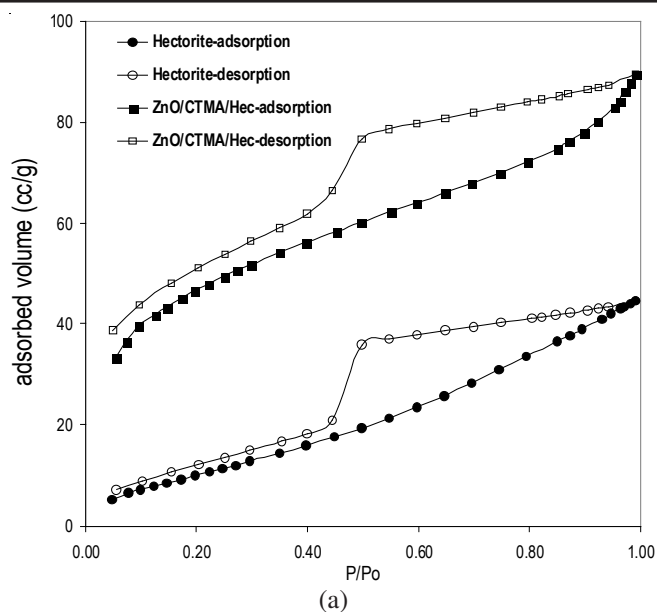
similar pattern indicate that no ZnO crystalline phase detected from XRD analysis. To ensure ZnO attachment in the material, elemental analysis data performed by using EDX analysis and the result is listed in Table-1.

Component	Content (% wt.)	
	Hectorite	ZnO/CTMA/Hec
SiO ₂	29.67	26.87
MgO	61.62	57.97
Na ₂ O	1.50	1.09
Li	0.06	0.04
ZnO	–	6.67

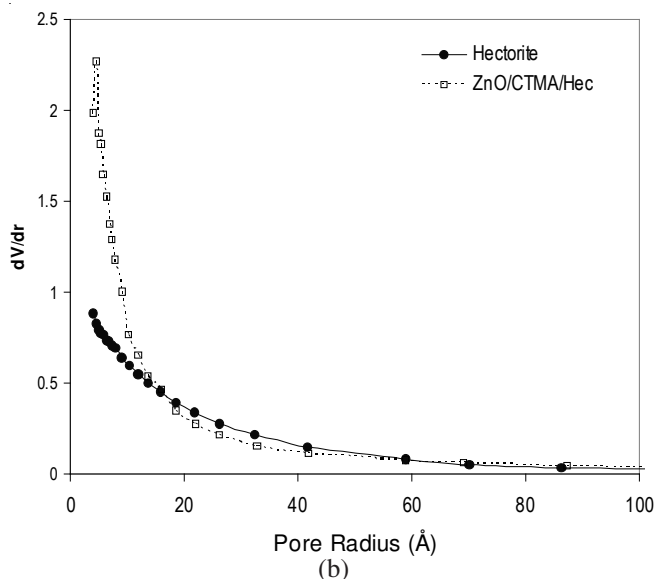
Content of ZnO in the ZnO/CTMA/Hec is 6.67 % which means less than 20 % of the Zn precursor stuck from the precursor solution of the dispersion process. The low Zn content compared to initial concentration as in precursor is probably made by the hydrophobic nature of CTMA pre-intercalated hectorite so that the equilibrium in its interaction with Zn precursor was occurred in less intensive.

The success of this ZnO dispersion is also verified from the change in surface profile data obtained by gas sorption analysis. Adsorption-desorption profile indicating improvement of N₂ adsorption capability is presented (Fig. 3). By using the isotherm, BET specific surface area, pore radius (BJH method) and pore volume of both hectorite and ZnO/CTMA/Hec showed the increased value, in that specific surface area of hectorite was 77.80 m²/g and increased to 224.42 m²/g after preparation as tabulated in Table-2. Pore size distribution curve (Fig. 3b) showing extremely significant change in micropores distribution of ZnO/CTMA/Hec compared to hectorite suggest that new micropores size were created during the modification.

Fig. 4 shows the kinetic curve of alizarin red S photo-oxidation by ZnO/CTMA/Hec, bulk-ZnO and hectorite with initial concentration of alizarin red S of 4.5×10^{-5} M and under the condition of 4 g/L catalyst concentration and H₂O₂



(a)



(b)

Fig. 3. (a) Adsorption-desorption profile of hectorite and ZnO/CTMA/Hec (b) Pore distribution curve of hectorite and ZnO/CTMA/Hec

Surface parameter	Content (% wt.)	
	Hectorite	ZnO/CTMA/Hec
Specific surface area (m ² /g)	77.80	224.42
Pore volume (cc/g)	9.56×10^{-3}	3.91×10^{-2}
Pore radius	11.33 Å	9.75 Å

concentration was 1.0×10^{-5} M in comparison with uncatalyzed condition. From the kinetic curve, it is seen that ZnO/CTMA/Hec photo-catalyzed reaction express the extremely improved photo-oxidation rate as shown by very rapid decreasing alizarin red S concentration start at of 15 min time of treatment.

Degradation rate of prepared material is higher respect to degradation rate using bulk-ZnO, hectorite and un-photo-catalyzed reaction. The lower rate of hectorite photocatalyzed reaction compared to as catalyzed by ZnO/CTMA/Hec is due

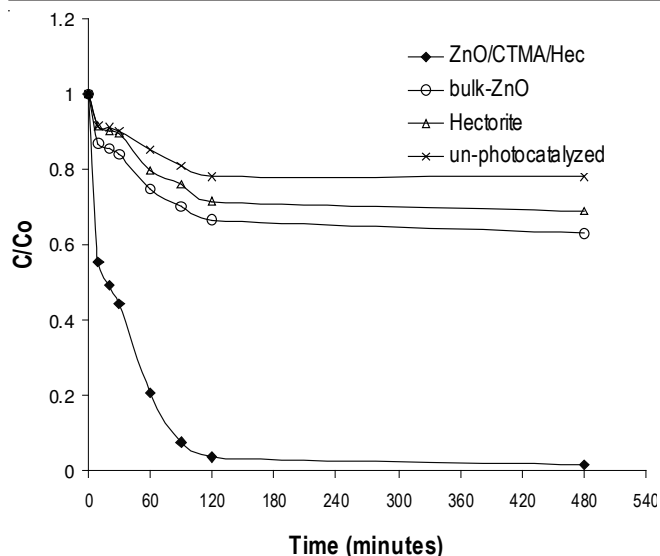


Fig. 4. Kinetic curve of alizarin red S degradation using prepared material compared with bulk-ZnO, hectorite

to the absence of photoactive material in catalyst so there is no radical formed by catalyst during its interaction with photon from UV lamp. Decreasing concentration was caused by adsorption process by catalyst. This reason is the most common reason for non-photoactive support as reported by some research comparing photo-activity of supported semiconductor material and the solid support²¹. As stated by the basic mechanism of heterogeneous photocatalysis, adsorption step of reactant into photocatalyst strongly affects the degradation rate, the influence of specific surface area to the rate is considered. Table-3 listed the specific surface area data and kinetic constant of each reaction condition presented by Fig. 4. Although bulk-ZnO has only 27.33 m²/g of specific surface area which was lower respect to hectorite, but it has photoactivity as shown by higher kinetic constant compared to hectorite and un-photocatalyzed condition. ZnO/CTMA/Hec has the highest photoactivity ($k = 5.54 \times 10^{-6}$ M/min). The combination of adsorption and photocatalysis mechanism was occurred during the treatment using ZnO/CTMA/Hec. This explanation is refer to the specific surface area of ZnO/CTMA/Hec which is much higher compared with hectorite and bulk-ZnO (224.42 m²/g).

Material	Kinetic constant (k/M min ⁻¹)	Specific surface area (m ² /g)
Hectorite	1.43×10^{-6}	77.80
ZnO/CTMA/Hec	5.54×10^{-6}	224.42
ZnO	1.78×10^{-6}	27.33
Un-photocatalyzed	1.14×10^{-6}	-

Effect of ZnO/CTMA/Hec dosage to the kinetic is studied by varying catalyst dosage in the alizarin red S photo-oxidation. Kinetic curve and plot of the influence of catalyst dosage is presented in Fig. 5. From the curve, it is concluded that at the dosage range of 0.5-4.0 g/L, photocatalyst addition leads to increase the degradation rate. The more higher photocatalyst

dosage, the more photoactive sites and surface area to promote radicals in solution system.

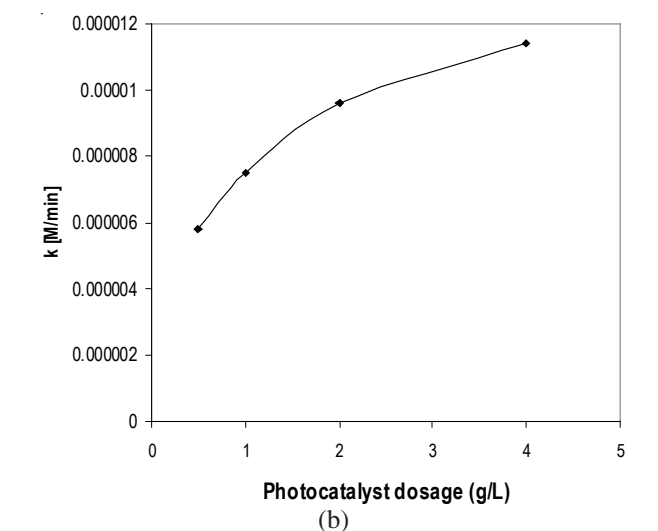
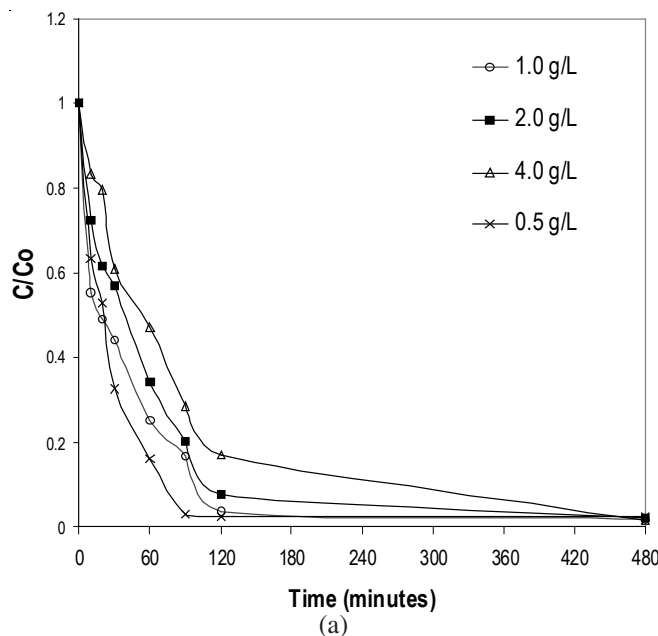


Fig. 5. (a) Kinetic curve of alizarin red S degradation in varied photocatalyst concentration (b) Correlation curve of kinetic constant vs. photocatalyst dosage

Conclusion

ZnO/CTMA/Hec was successfully prepared from hectorite as shown by improving physico-chemical character of material. The immobilization of ZnO *via* CTMA pre-intercalation does not give effect to the support crystallinity, moreover specific surface area of material increased from 77.80 m²/g to 224.42 m²/g. These characters lead to the increasing photo-activity explained by kinetics data in alizarin red S photo-oxidation.

ACKNOWLEDGEMENTS

The authors gratefully thank to DPPM Universitas Islam Indonesia for financial support through Research Grant Hibah Penelitian Dasar UII 2011.

REFERENCES

1. K. Rajeshwar, M.E. Osugi, W. Chanmanee, C.R. Chenthamarakshana, M.V.B. Zanoni, P. Kajitvichyanukul and R. Krishnan-Ayer, *J. Photochem. Photobiol. C: Photochem. Rev.*, **9**, 171 (2008).
2. J.M. Tatibouet, E. Guelou and J. Fourmier, *Topics Catal.*, **33**, 1 (2005).
3. N. Genç and E. Can-Dogan, *Polish J. Environ. Stud.*, **15**, 73 (2006).
4. J.H. Heredia, J. Torregrosa, J.R. Dominguez and J.A. Peres, *J. Hazard. Mater.*, **B83**, 255 (2001).
5. K. Byrappa, A. Subramani, S. Ananda, S.L. Rai, M.H. Sunita, B. Basavignu and L. Rai, *J. Mater. Sci.*, **41**, 1355 (2006).
6. M. Anpo, *Bull. Chem. Soc. (Japan)*, **77**, 1427 (2004).
7. N. Agoudjil and T. Benkancem, *Desalination*, **206**, 537 (2007).
8. N. Satoh, T. Nakashima, K. Kamikura and Y. Yamamoto, *Nature Nanotechnol.*, **3**, 106 (2008).
10. V.K. Ivanov, A.S. Shaporev, F.Y. Sharikov, and A.Y. Baranchikov, *Superlatt. Microstruct.*, **42**, 421 (2006).
9. S.S. Katkar, P.H. Mohite, L.S. Gadekar, B.R. Arbad and M.K. Lande, *Green Chem. Lett. Rev.*, **3**, 287 (2010).
10. M.A. Behnajady, N. Modirshahla, N. Daneshvar and M. Rabbani, *J. Hazard. Mater.*, **140**, 257 (2006).
11. R. Anedda, C. Cannas, A. Musinu, G. Pinna, G. Piccaluga and H. Casu, *J. Nanopart. Res.*, **10**, 107 (2008).
12. G.D. Mihai, V. Meynen, M. Mertens, N. Bilba, P. Cool and E.F. Vansant, *J. Mater. Sci.*, **45**, 5786 (2010).
13. Q. Lu, Z. Wang, J. Li, P. Wang and X. Ye, *Nanoscale Res. Lett.*, **4**, 646 (2009).
14. K. Mogyorosi, J. Nemeth, I. Dekany and J.H. Fendler, *Adsorp. Nanostruct. Progr. Colloid Polym. Sci.*, **117**, 88 (2003).
15. T.S. Anirudhan and M. Ramachandran, *Appl. Clay Sci.*, **35**, 276 (2007).
16. G.W. Beall, *Appl. Clay Sci.*, **24**, 11 (2003).
17. S. Baldassari, S. Komarneni, E. Mariani and M. Villa, *Appl. Clay Sci.*, **31**, 134 (2005).
18. A. Kajbafvala, S. Zanganeh, E. Kajbafvala, H.R. Zargar, M.R. Bayati and S.K. Sadreza, *J. Alloys Comp.*, **497**, 325 (2010).
19. T. Krishnakumar, R. Jayaprakash, N. Pinna, V.N. Singh, B.R. Mehta and A.R. Phani, *Mater. Lett.*, **63**, 242 (2009).
20. S. Yapar, *Colloids Surfaces A: Physicochem. Eng. Aspects*, **345**, 75 (2009).
21. I. Fatimah, P. Shukla and F. Kooli, *J. Appl. Sci.*, **9**, 3715 (2009).